J. Fluid Mech. (2016), *vol.* 809, *pp.* 705–715. © Cambridge University Press 2016
doi:10.1017/jfm.2016.697

Hollow vortices in shear

Luca Zannetti[1,†], Michele Ferlauto[2] and Stefan G. Llewellyn Smith[3]

[1]Accademia delle Scienze di Torino, Via Accademia delle Scienze 6, 10123 Torino, Italy

[2]DIMEAS, Politecnico di Torino, Corso Duca degli Abruzzi 24, 10129 Torino, Italy

[3]Department of Mechanical and Aerospace Engineering, Jacobs School of Engineering, UCSD, 9500 Gilman Drive, La Jolla, CA 92093-0411, USA

(Received 10 June 2016; revised 22 September 2016; accepted 20 October 2016; first published online 16 November 2016)

An analytical method for determining the shape of hollow vortices in shear flows is presented in detail. In a non-dimensional formulation, it is shown that the problem has one degree of freedom represented by the free choice of the non-dimensionalized speed κ at the boundary of the vortex. The solutions form two families of shapes corresponding to vortex circulation and shear-flow vorticity having the opposite or same sign. When the signs are opposite, the shape family resembles that described by Llewellyn Smith & Crowdy (*J. Fluid Mech.*, vol. 691, 2012, pp. 178–200) for hollow vortices in a potential flow with strain. As for that flow, there is a minimum value of κ below which there is no solution as the boundary of the vortex self-intersects, while, when the signs are the same, solutions exist for $0 < \kappa$.

Key words: vortex dynamics, vortex flows

1. Introduction

The study of two-dimensional vortices in a non-uniform background flow has attracted the attention of many researchers in vortex dynamics because of its overall theoretical importance and its many applications such as, for instance, flow control, geophysical flows, turbulence. To this purpose, several vortex models have been adopted, in particular point vortices, vortex patches and hollow vortices.

In the context of the detection of aircraft wakes, Moore & Saffman (1971) studied the shape of finite-area vortices in a two-dimensional inviscid straining flow. They considered irrotational strain and simple shear. By modelling vortices as vortex patches, i.e. as regions with constant vorticity, $\omega = \text{const}$, they found steady configurations with elliptical shapes. Kida (1981) showed analytically that the Moore & Saffman (1971) solutions are particular steady cases of more general unsteady time-periodic solutions, in which, depending on the shear intensity, vortices rotate preserving their elliptical shape and varying their ellipticity. Earlier, Chaplygin and Kirchhoff had found solutions for (i) the motion of an elliptical patch of uniform vorticity in an exterior field of pure shear; (ii) the motion of a (symmetric or non-symmetric) dipolar vortex with a continuous distribution of vorticity translating steadily along a straight path; and (iii) the motion of a non-symmetric vortex dipole moving along a circular trajectory (Lamb 1932; Meleshko & van Heijst 1994).

† Email address for correspondence: luca.zannetti@polito.it

Schecter & Dubin (2001) examined two-dimensional vortex motion in a shear flow with non-uniform vorticity. In general, a vortex travels to an extremum in the background vorticity distribution and the rate of this migration increases with the magnitude of the background vorticity gradient. They also found that a retrograde vortex, which rotates against the local shear, moves orders of magnitude faster than a prograde vortex of equal strength.

Besides the general interest in exact solutions of the Euler equations for non-trivial flows, analytical models of vortical structures in shear flows are relevant to the Earth's atmosphere and oceans. Jupiter's Great Red Spot is another example connected to the present study on hollow vortices: the Great Red Spot is a vortical structure that interacts with a shear flow and exhibits high vorticity in its outer region and low vorticity in its core (see Shetty, Asay-Davis & Marcus (2010), and references therein). Vorticity has also been put forward as a mechanism in the formation of the Solar system (Tanga *et al.* 1996).

More recently, Llewellyn Smith & Crowdy (2012) solved a problem related to the Moore & Saffman (1971) problem of vortex equilibrium in a straining flow using the hollow-vortex model that takes that the inside of the vortex to be vacuum or, equivalently, a zero-vorticity region bounded by a vortex sheet (in both cases, at steady state, a constant pressure inside the core requires a constant speed at the vortex boundary). They limited their study to the irrotational strain case and provided a closed-form analytical solution for steady configurations.

In the present study, we enrich the scenario by giving analytical solution to the problem of finding the shape a hollow vortex takes in equilibrium in a shear flow.

Zero vorticity, $\omega = 0$, means that the streamfunction ψ is harmonic in the inside of the vortex. When the flow is steady, ψ is constant at the boundary and, according to the maximum principle, ψ is constant throughout the inside of the vortex. It follows that flow velocity is zero and pressure is constant in the interior. Equilibrium then requires constant flow speed along the exterior side of the bounding vortex sheet. The determination of the shape of a hollow vortex is so reduced to a free-streamline problem, whose study goes back to 19th century and Kirchhoff free-streamline theory. Birkhoff & Zarantonello (1957) and Gurevich (1966) present a broad survey of this problem. Hicks (1883) and Pocklington (1895) are examples of historic solutions for hollow-vortex shapes. More recent studies on hollow vortices, based on the classical hodograph method or more innovative methods, have been produced. Among many references on the matter, one can mention, for instance, Baker, Saffman & Sheffield (1976), Lin & Landweber (1977), Crowdy & Green (2011), Telib & Zannetti (2011), Crowdy, Llewellyn Smith & Freilich (2012), Elcrat & Zannetti (2012), Llewellyn Smith & Crowdy (2012), Zannetti & Lasagna (2013), Elcrat, Ferlauto & Zannetti (2014), Green (2015).

Once the problem is non-dimensionalized, we show that the problem has one degree of freedom, i.e. the solution depends on a single non-dimensional parameter. The solutions form two separate families related to opposite or same sign of shear vorticity and vortex circulation.

When shear vorticity and vortex circulation are opposite, the solutions are analogous to and have the same flow topology as the hollow vortices in an irrotational straining flow studied by Llewellyn Smith & Crowdy (2012). We have selected as free parameter the non-dimensional speed κ of the flow at the boundary of the vortex. As $\kappa \to \infty$ the solution is a point vortex. For large finite values of κ the point vortex is desingularized into a finite-area vortex. As κ decreases, the vortex area increases until a maximum area is reached and then decreases. Unlike the solution of Llewellyn

Smith & Crowdy (2012), our solution is not expressed in closed form but is obtained by a root-finding process.

In the family corresponding to the same sign of shear-flow vorticity and vortex circulation, the point-vortex solution is, as above, obtained for $\kappa \to \infty$. The vortex area increases monotonically as κ decreases.

The study of stability of the solutions goes beyond the scope of the present study. However the present analytical method of solution offers a tool for further studies on this important aspect of the problem, following on from, for example, the linear stability analysis described by Llewellyn Smith & Crowdy (2012) for hollow vortices in a potential strained flow or by Crowdy *et al.* (2012) for Pocklington's vortex pair.

2. Hollow-vortex structure

We consider a hollow vortex in equilibrium in a two-dimensional (2-D) incompressible flow governed by the Euler equation. Then

$$\nabla^2\psi = -\omega, \tag{2.1}$$

where ψ denotes the streamfunction and ω, which is constant, the vorticity of the flow past the vortex. At infinity the flow tends to a pure shear flow, that is,

$$\nabla_\perp\psi \to -\omega y\boldsymbol{i} \quad \text{as } (x, y) \to \infty, \tag{2.2}$$

where (x, y) are Cartesian coordinates and $\boldsymbol{i}$ is the unit vector along the x-axis.

The vorticity inside the vortex is assumed to be zero. As a consequence, the internal flow is at rest, the pressure is constant at the vortex boundary and, according to Bernoulli's equation, the vortex boundary is a vortex sheet with constant speed $q = k$ on the external side. Steady flow and constant tangential velocity result in

$$\frac{\partial\psi}{\partial s} = 0, \quad \left|\frac{\partial\psi}{\partial n}\right| = k \quad \text{on the boundary}, \tag{2.3a,b}$$

where n and s are normal and tangential directions at the boundary.

This is a free-boundary problem which requires finding the vortex shape that satisfies the above conditions. For the sake of simplicity, a summary description of the solution is presented in this section while a detailed description is given in the appendices.

Briefly, the solution is obtained according to the classical conformal mapping method. Let $z = x + \mathrm{i}y$ be the complex coordinate in the physical z-plane of motion and $\zeta = \xi + \mathrm{i}\eta$ the complex coordinate in a transformed ζ-plane. The solution consists in finding the function $z = z(\zeta)$ mapping the unit circle in the ζ-plane onto the vortex contour in the z-plane.

For flow regularity, the mapping $z(\zeta)$ has to be analytic outside the unit circle of the ζ-plane and such that $\lim_{\zeta\to\infty} z(\zeta) = \infty$ and the mapping derivative $\mathrm{d}z/\mathrm{d}\zeta$ has to be analytic and different from zero. Thus, $\mathrm{d}z/\mathrm{d}\zeta$ can be expressed as

$$\frac{\mathrm{d}z}{\mathrm{d}\zeta} = \exp\sum_{n=1}^{\infty} b_n\zeta^{-(n-1)}. \tag{2.4}$$

Once the coefficients b_n are determined by the solution process, the mapping $z(\zeta)$ is obtained by analytic integration, as shown in the appendices.

In general, (2.1) is satisfied by the streamfunction

$$\psi(z(\zeta)) = \psi_\omega + \psi_p = -\frac{\omega}{2}\mathrm{Im}^2[z(\zeta)] + \mathrm{Im}[w_p(\zeta)], \tag{2.5}$$

where the first term ψ_ω is the streamfunction of a pure shear flow whose constant vorticity is ω and the second term ψ_p is the streamfunction of an irrotational flow whose complex potential is w_p. Continuing, (2.2) is satisfied by setting

$$w_p = \frac{\gamma}{2\pi \mathrm{i}} \log \zeta - G(\zeta). \tag{2.6}$$

The complex potential $w_p(\zeta)$ is made up of the combination of the complex potential of a point vortex with circulation γ located on the origin of the ζ-plane and a complex potential $G(\zeta)$ which is analytic for $|\zeta| \geqslant 1$ and is finite at infinity. Hence, in general, the latter can be written as

$$G(\zeta) = \sum_{n=1}^{\infty} c_n \zeta^{-(n-1)}. \tag{2.7}$$

As detailed in the appendices, for given values of vorticity ω, point-vortex circulation γ and vortex-contour speed k, the coefficients b_n, c_n of the above series, truncated at a suitably large value N, are determined by enforcing the constraints (2.3).

According to (2.5) and (2.6), Stokes' theorem and the residue theorem, the circulation Γ of the hollow vortex is

$$\Gamma = \oint_\partial \boldsymbol{q} \cdot \mathrm{d}\boldsymbol{s} = kL_c = \oint_\partial \left(\frac{\partial \psi_\omega}{\partial y}\mathrm{d}x - \frac{\partial \psi_\omega}{\partial x}\mathrm{d}y \right) + \mathrm{Re} \oint_{|\zeta|=1} \frac{\mathrm{d}w_p}{\mathrm{d}\zeta}\,\mathrm{d}\zeta = \omega A_v + \gamma, \tag{2.8}$$

where A_v is the vortex area and L_c is the vortex perimeter.

Let the problem be non-dimensionalized by taking the absolute value of the vorticity of the shear flow ω as reference vorticity ($\omega_{ref} = |\omega|$) and the absolute value of the vortex circulation $\gamma/(2\pi)$ as the reference circulation ($\gamma_{ref} = |\gamma/(2\pi)|$). The reference length and velocity become $l_{ref} = \sqrt{|\gamma/(2\pi\omega)|}$ and $q_{ref} = \sqrt{|\omega\gamma/(2\pi)|}$, respectively.

The streamfunction of the non-dimensionalized problem, written as function of ζ, becomes

$$\psi(\zeta) = -\frac{\delta}{2}\mathrm{Im}^2[z(\zeta)] - \tau \log|\zeta| - \mathrm{Im}[G(\zeta; \delta, \tau, \kappa)], \tag{2.9}$$

with $\delta = \mathrm{sgn}(\omega)$, $\tau = \mathrm{sgn}(\gamma)$ and where

$$\kappa = \frac{k}{\sqrt{|\omega\gamma/(2\pi)|}}, \tag{2.10}$$

is the non-dimensional velocity at the vortex boundary. For $\delta = \tau$ and $\delta = -\tau$, two families of shapes are defined by varying the parameter κ. That is, all the solutions corresponding to given values of vorticity ω and circulation γ can be scaled onto two family of shapes.

As for Llewellyn Smith & Crowdy (2012), the general topology of the flow can be deducted by considering the related problem of a point vortex in the same shear flow. In the physical z-plane, the non-dimensionalized streamfunction for the point-vortex flow is

$$\psi_{pv} = -\frac{\delta}{2}y^2 - \frac{\tau}{2}\log(x^2 + y^2). \tag{2.11}$$

Figure 1(*a*) shows the streamline pattern for $\delta = -\tau$, that is for a point vortex whose circulation is opposite to the shear vorticity. The flow has two stagnation points and a separatrix that divides a finite body of recirculating fluid entrained by the vortex from the external non-recirculating flow driven by the shear flow.

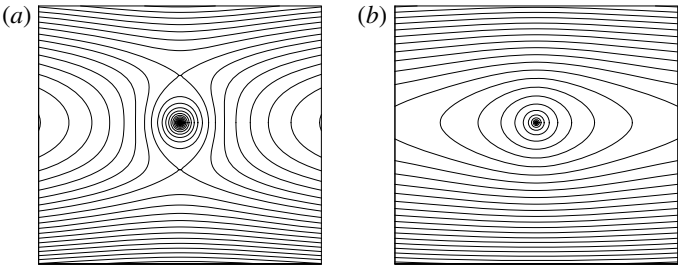

FIGURE 1. Streamline patterns of the point-vortex solution: (*a*) $\delta = -\tau$; (*b*) $\delta = \tau$.

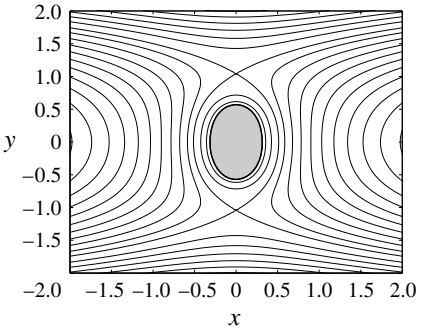

FIGURE 2. Hollow-vortex streamlines for $\delta = -\tau$ and $\kappa = 2$.

Figure 1(*b*) shows the case of equal sign point-vortex circulation and shear vorticity ($\delta = \tau$). There are no stagnation points and all the streamlines are closed. Close to the point vortex the streamline shapes are near circular, while far away the shear flow makes them increasingly elongated.

2.1. *The* $\delta = -\tau$ *case*

We first consider the solutions for $\delta = -\tau = -1$ for different values of κ. It is obvious that the $\delta = -\tau = 1$ choice generates the same flows streaming in reversed direction.

An example solution is provided by figure 2 where the flow field has been drawn for $\kappa = 2$. By varying the parameter κ, a hollow-vortex solution can be continued onto a family of vortices with different shapes and areas. Hollow-vortex shapes are displayed in figure 3(*a*) for given values of the non-dimensionalized speed κ in the range $1.32 \leqslant \kappa$. As $\kappa \to \infty$ the solution tends to a zero-area vortex, that is, to the point-vortex solution. As κ decreases the point vortex is desingularized into more and more elongated vortices with finite area. The non-dimensional area $\alpha = A_v/l_{ref}^2$ is plotted versus κ in figure 3(*b*). For $\kappa = \kappa^\star \approx 1.6$, the vortex area reaches a maximum. As κ decreases, the shapes start to resemble those computed by Llewellyn Smith & Crowdy (2012) for hollow vortices in a strain flow ($n = 2$ in their notation; see their figures 2 and 3), with a limiting value for κ below which there is no solution as the boundary starts to self-intersect. This outcome is expected for $\kappa < \kappa^\star$, where a decrease of speed at the vortex contour is accompanied by a decrease of the vortex area. In non-dimensional form (2.8) yields $\kappa l_c = 2\pi\tau + \delta\alpha$, where l_c is the non-dimensional length of the vortex contour. In the present case $\delta = -\kappa = -1$ and the contour length becomes $l_c = (2\pi - \alpha)/\kappa$. As κ decreases it becomes longer and, since the vortex

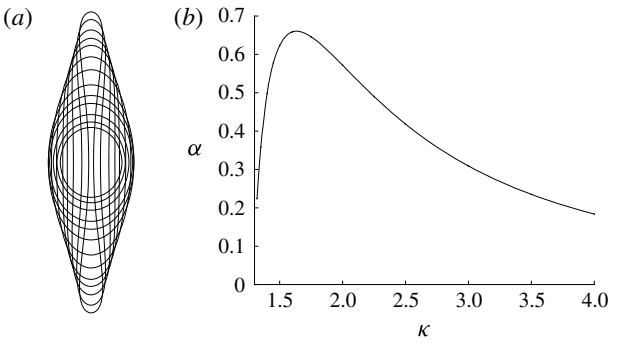

FIGURE 3. Hollow vortices for $\delta = -\tau$. (*a*) Vortex shapes for $\kappa = 1.4$, 1.5, 1.6, 1.75, 2, 2.25, 2.5, 3, 3.5, 4; (*b*) non-dimensionalized vortex area versus κ.

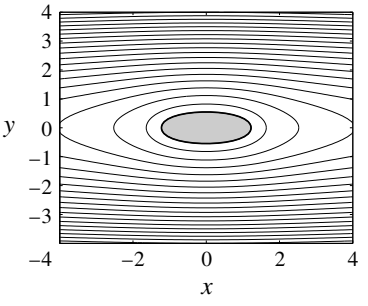

FIGURE 4. Streamline pattern for $\delta = \tau$ and $\kappa = 1.5$.

area is getting smaller, it will eventually self-intersect. The pinch-off happens between $\kappa = 1.32$ and $\kappa = 1.31$ (the numerical procedure will produce self-intersecting shapes as κ continues to decrease). An explanation of such an agreement might be given by noticing that a shear flow can be decomposed into a strain flow plus a rigid body rotation: $\psi_{sh} = \psi_{st} + \psi_{\omega}$, with

$$\psi_{sh} = -(\omega/2)y^2, \quad \psi_{st} = (\omega/4)(x^2 - y^2) \quad \text{and} \quad \psi_{\omega} = -(\omega/4)(x^2 + y^2), \qquad (2.12a\text{–}c)$$

and that the streamline pattern for a hollow vortex in a strain flow has the same topology as for a $\delta = -\tau$ hollow vortex in a shear flow (see figure 2). By taking a normalization analogous to the present one for the problem examined by Llewellyn Smith & Crowdy (2012), that is by selecting, according to their notation, the strain factor γ and the vortex circulation Γ as reference values, a non-dimensionalized speed $\tilde{\kappa}$ of the vortex contour can be defined which results in a monotonically decreasing function of the parameter μ used in their study. As a consequence, the behaviour of area versus μ in their figure 3(*b*) has the same behaviour of our plot of area versus κ shown by the present figure 3.

2.2. *The* $\delta = \tau$ *case*

Figure 4 shows the streamline pattern for $\delta = \tau = 1$ and for $\kappa = 1.5$. As discussed above, this solution appears as a desingularization of the point-vortex solution shown in figure 1(*b*). The entire flow field consists of closed streamlines and there are

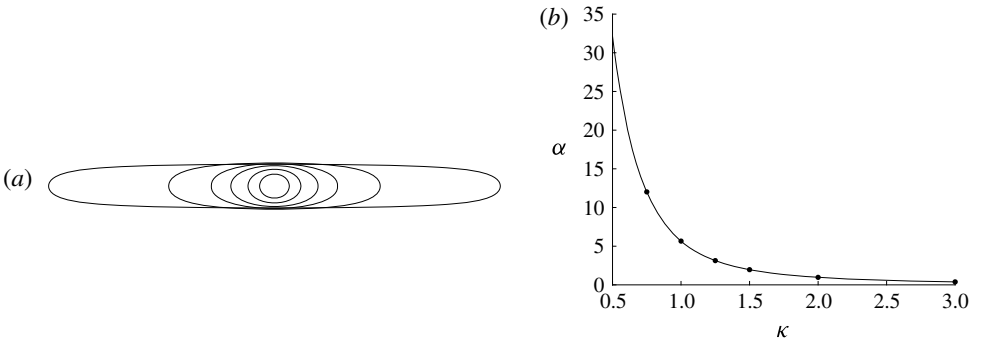

FIGURE 5. Hollow vortices for $\delta = \tau$. (*a*) Vortex shapes for $\kappa = 0.75$, 1, 1.25, 1.5, 2, 3; (*b*) non-dimensionalized vortex area versus κ.

no stagnation points. By varying the vortex contour speed κ, the solution can be continued to vortices with different areas. Vortex shapes are drawn for given values of κ in figure 5(*a*), the corresponding area values are plotted on figure 5(*b*). As $\kappa \to \infty$ the solution tends to a zero-area vortex, that is, to the point-vortex solution. As κ decreases the vortex shape elongates and the area increases. The limit as $\kappa \to 0$ is an infinite stagnant strip above and below bounded by two shear flows with zero velocity at the strip boundary. This is reminiscent of the limit of the solution of Baker *et al.* (1976) when the vortices in the array start to touch and the array reduces to a strip.

3. Concluding remarks

The paper presents in detail an analytical method for determining the shape of hollow vortices in shear flows.

In a non-dimensional formulation, it is shown that the problem has one degree of freedom represented by the free choice of the non-dimensional flow speed κ at the vortex contour. For $\kappa \to \infty$ the solution tends to the point-vortex flow. For finite values of κ, the solution is desingularized into finite-area vortices. The solutions form two families of shapes which correspond to vortex circulation and shear-flow vorticity having opposite sign ($\gamma\omega < 0$) or equal sign ($\gamma\omega > 0$).

For $\gamma\omega < 0$ the family of shapes resembles that described by Llewellyn Smith & Crowdy (2012) for hollow vortices in strained potential flows. As for that family, there is a value of κ for which the vortex area reaches a maximum, and there is also a minimum value of κ below which there is no solution as the vortex contour self-intersects.

For $\gamma\omega > 0$, the area of the vortex is a monotonic decreasing function of κ. For $\kappa \to \infty$ the solution tends to the zero-area point vortex. Solutions exist for arbitrary small values of κ and that for $\kappa \to 0$ the vortex shape tends to an infinite strip.

The method intrinsically looks for steady solutions, thus oscillating solutions à la Kida (1981) are not considered and cannot be excluded.

Acknowledgements

The authors would like to thank D. Freilich for carrying out calculations to verify the results for small values of κ.

Appendix A. Coefficient series determination

The series coefficients b_n and c_n in (2.4) and (2.7) are computed by a fixed-point iteration or zero-finding process.

According to (2.9) and (2.6), the complex velocity $u - \mathrm{i}v$, written as a function of ζ, is

$$u - \mathrm{i}v = -\delta \mathrm{Im}[z(\zeta)] - \left(\frac{\mathrm{i}\tau}{\zeta} + \frac{\mathrm{d}G}{\mathrm{d}\zeta}\right)\frac{1}{\mathrm{d}z/\mathrm{d}\zeta}. \tag{A 1}$$

Let $\tilde{u}$ and $\tilde{v}$ be the normal and tangential components of the flow velocity at the vortex boundary, the complex velocity $\tilde{u} - \mathrm{i}\tilde{v}$ becomes

$$\tilde{u} - \mathrm{i}\tilde{v} = \left[(u - \mathrm{i}v)\frac{\mathrm{d}z/\mathrm{d}\zeta}{|\mathrm{d}z/\mathrm{d}\zeta|}\zeta\right]_{|\zeta|=1}. \tag{A 2}$$

We assume that τ is positive ($\tau = 1$), as a consequence $\tilde{v}$ is positive and conditions (2.3) become $\tilde{u} = 0$ and $\tilde{v} = \kappa$, that is

$$\mathrm{Re}\left(\frac{\mathrm{d}G}{\mathrm{d}\zeta}\zeta\right)_{|\zeta|=1} = \mathrm{Re}\left[-\delta \mathrm{Im}(z(\zeta))\frac{\mathrm{d}z}{\mathrm{d}\zeta}\zeta\right]_{|\zeta|=1} \tag{A 3}$$

and

$$\left|\frac{\mathrm{d}z}{\mathrm{d}\zeta}\right| = \left\{\frac{\mathrm{Im}[\delta \mathrm{Im}(z(\zeta))\zeta\,\mathrm{d}z/\mathrm{d}\zeta + \zeta\,\mathrm{d}G/\mathrm{d}\zeta] + \tau}{\kappa}\right\}_{|\zeta|=1}. \tag{A 4}$$

Let the series (2.4), (2.7) be truncated at a suitably large value $n = N$ (in our computations we have set $N = 128$). The process is started by assuming a set of values for the b_n coefficients. A starting guess of $b_n = 0$ for $n = 1, \ldots, N$ for the largest value of κ was used, after which κ was decreased and the previous value of b_n was used as the starting guess. As shown below, (A 3) allows the computation of a first set of c_n coefficients, then (A 4) allows the coefficients b_n to be updated. The process is repeated until the absolute maximum difference between old and new values of the coefficients b_n falls below a given threshold D (we set $D = 10^{-10}$). For large enough values of κ (around 1.5 for the case $\delta = -\tau$ and 1.2 for the case $\delta = \tau$), a fixed-point iteration was used in which the new values of b_n replace the old. For smaller values of κ, a multidimensional root-finding algorithm (`fsolve` in Matlab) is used to find zeros of the difference between old and new coefficients.

For $|\zeta| = 1$, so that $\zeta = \mathrm{e}^{\mathrm{i}\varphi}$, (A 3) can be recast as

$$\mathrm{Re}\left[\sum_{n=1}^{N} C_n \mathrm{e}^{-\mathrm{i}(n-1)\varphi}\right] = \mathrm{Re}\left[-\delta \mathrm{Im}(z(\zeta))\frac{\mathrm{d}z}{\mathrm{d}\zeta}\zeta\right]_{|\zeta|=1}, \tag{A 5}$$

with $C_n = -(n-1)c_n$. Once old values of the right-hand side are evaluated at $2N$ equispaced points of the ζ-plane unit circle, the computation of a new set of c_n ($n \neq 1$) coefficients can be obtained through the discrete Fourier transform. The coefficient c_1 is an additive constant to the potential $G(\zeta)$ (2.7) which can be arbitrarily chosen.

Then (2.4) yields

$$\log\left|\frac{\mathrm{d}z}{\mathrm{d}\zeta}\right| = \mathrm{Re}\left(\sum_{n=1}^{N} b_n \zeta^{-(n-1)}\right) \tag{A 6}$$

and (A 4) can be recast as

$$\mathrm{Re}\left(\sum_{n=1}^{N} b_n \mathrm{e}^{-\mathrm{i}(n-1)\varphi}\right) = \log\left\{\frac{\mathrm{Im}[\delta \mathrm{Im}(z(\zeta))\zeta\, \mathrm{d}z/\mathrm{d}\zeta + \zeta\, \mathrm{d}G/\mathrm{d}\zeta] + \tau}{\kappa}\right\}_{|\zeta|=1}. \quad \text{(A 7)}$$

A new set of values for b_n is obtained by the discrete Fourier transform of the right-hand side evaluated at $2N$ equispaced points of the ζ-plane unit circle by means of the old b_n values, needed to evaluate the $z(\zeta)$ and $\mathrm{d}z/\mathrm{d}\zeta$ terms, and by means of the updated c_n coefficients, needed to evaluate the $\mathrm{d}G/\mathrm{d}\zeta$ term.

The mapping $z(\zeta)$ is given by the indefinite integral $z(\zeta) = \int (\mathrm{d}z/\mathrm{d}\zeta)\, \mathrm{d}\zeta$, that is

$$z(\zeta) = \int \exp \sum_{n=1}^{N} b_n \zeta^{-(n-1)} \mathrm{d}\zeta. \quad \text{(A 8)}$$

The Laurent series expansion of the integrand yields

$$\exp \sum_{n=1}^{N} b_n \zeta^{-(n-1)} \equiv \sum_{n=1}^{N} a_n \zeta^{-(n-1)}. \quad \text{(A 9)}$$

We show below that there is a closed-form analytic relationship between the coefficients a_n and b_n having the form $a_j = f(b_1, \ldots, b_j)$. Since the closure condition of the vortex implies that $\oint (\mathrm{d}z/\mathrm{d}\zeta)_{|\zeta|=1} \mathrm{d}\zeta = 2\pi \mathrm{i} a_2 = 0$, the integral (A 8) is

$$z(\zeta) = a_1 \zeta - \sum_{n=3}^{N} \frac{a_n}{n-2} \zeta^{-(n-2)}. \quad \text{(A 10)}$$

All the solutions here found are symmetric with respect to the x, y axes. As a consequence the computed a_n, b_n are all real and equal to zero for even n indexes.

Appendix B. The $a_j = f(b_1, \ldots, b_j)$ relationship

We set

$$\sigma = \exp s(t), \quad \text{(B 1)}$$

with

$$s = \sum_{n=1}^{N} b_n t^{n-1}. \quad \text{(B 2)}$$

For $t = 1/\zeta$, the identity (A 9) becomes

$$\sigma \equiv \sum_{n=1}^{N} a_n t^{n-1}. \quad \text{(B 3)}$$

The coefficients a_n can be found as coefficients of the McLaurin series expansion or, equivalently, as residues at $t = 0$ of σ, that is

$$a_n = \mathrm{Res}\left(\sigma \frac{1}{t^n}\right)_{t=0} = \frac{1}{(n-1)!}\left(\frac{\mathrm{d}^{n-1}}{\mathrm{d}t^{n-1}}\sigma\right)_{t=0}. \quad \text{(B 4)}$$

The first coefficient clearly is $a_1 = e^{b_1}$. The subsequent coefficients a_n are obtained by evaluating the right-end side of (B 4) with a recursion formula which avoids actual onerous derivations. In fact, the first derivative of σ is

$$\frac{d\sigma}{dt} = \sigma \frac{ds}{dt} \tag{B 5}$$

and, according to the general Leibniz rule for derivation of products, the higher-order derivatives result in

$$\frac{d^{j+1}\sigma}{dt^{j+1}} = \frac{d^j}{dt^j}\left(\sigma \frac{ds}{dt}\right) = \sum_{k=0}^{j} \frac{j!}{k!(j-k)!} \frac{d^k\sigma}{dt^k} \frac{d^{j-k+1}s}{dt^{j-k+1}}. \tag{B 6}$$

For $t = 0$, this gives $(d^j s/dt^j)_{t=0} = j! b_{j+1}$, thus the values of the σ derivatives are given by the recursion formula

$$\left(\frac{d^{j+1}\sigma}{dt^{j+1}}\right)_{t=0} = \sum_{k=0}^{j} \frac{j!}{k!} \left(\frac{d^k\sigma}{dt^k}\right)_{t=0} (j-k+1) b_{j-k+2}, \tag{B 7}$$

which, according to (B 4), yields

$$a_{j+1} = \frac{1}{j} \sum_{k=0}^{j-1} (j-k) a_{k+1} b_{j-k+1}, \quad \text{with } j = 1, 2, \ldots, N-1, \tag{B 8}$$

where the starting value is $a_1 = e^{b_1}$.

REFERENCES

BAKER, G. R., SAFFMAN, P. G. & SHEFFIELD, J. S. 1976 Structure of a linear array of hollow vortices of finite cross-section. *J. Fluid Mech.* **74**, 1469–1476.

BIRKHOFF, G. & ZARANTONELLO, E. H. 1957 *Jets, Wakes, and Cavities*. Academic.

CROWDY, D. G. & GREEN, C. C. 2011 Analytical solutions for von Kármán streets of hollow vortices. *Phys. Fluids* **23**, 126602.

CROWDY, D. G., LLEWELLYN SMITH, S. G. & FREILICH, D. V. 2012 Translating hollow vortex pairs. *Eur. J. Mech. (B/Fluids)* **37**, 180–186.

ELCRAT, A., FERLAUTO, M. & ZANNETTI, L. 2014 Point vortex model for asymmetric inviscid wakes past bluff bodies. *Fluid Dyn. Res.* **46**, 031407.

ELCRAT, A. & ZANNETTI, L. 2012 Models for inviscid wakes past a normal plate. *J. Fluid Mech.* **708**, 377–396.

GREEN, C. C. 2015 Analytical solutions for two hollow vortex configurations in an infinite channel. *Eur. J. Mech. (B/Fluids)* **54**, 69–81.

GUREVICH, M. I. 1966 *Theory of Jets in Ideal Fluids*. Academic.

HICKS, W. M. 1883 On the steady motion of a hollow vortex. *Proc. R. Soc. Lond.* **35**, 304–308.

KIDA, S. 1981 Motion of an elliptic vortex in a uniform shear flow. *J. Phys. Soc. Japan* **50**, 3517–3520.

LAMB, H. 1932 *Hydrodynamics*, 6th edn. Cambridge University Press.

LIN, A. & LANDWEBER, L. 1977 On a solution of the Lavrentiev wake model and its cascade. *J. Fluid Mech.* **79**, 801–823.

LLEWELLYN SMITH, S. G. & CROWDY, D. G. 2012 Structure and stability of hollow vortex equilibria. *J. Fluid Mech.* **691**, 178–200.

MELESHKO, V. V. & VAN HEIJST, G. J. F. 1994 On Chaplygin's investigations of two-dimensional vortex structures in an inviscid fluid. *J. Fluid Mech.* **272**, 157–182.

MOORE, D. W. & SAFFMAN, P. G. 1971 Structure of a line vortex in an imposed strain. In *Aircraft Wake Turbulence and its Detection* (ed. J. A. Olsen, A. Goldburg & M. Rogers), pp. 339–354. Plenum.

POCKLINGTON, H. C. 1895 The configuration of a pair of equal and opposite hollow straight vortices, of finite cross-section, moving steadily through fluid. *Proc. Camb. Phil. Soc.* **8**, 178–187.

SCHECTER, D. A. & DUBIN, D. H. E. 2001 Theory and simulations of two-dimensional vortex motion driven by a background vorticity gradient. *Phys. Fluids* **13** (6), 1704–1723.

SHETTY, S., ASAY-DAVIS, X. S. & MARCUS, P. S. 2010 On the interaction of Jupiter's great red spot and zonal jet streams. *J. Atmos. Sci.* **64**, 4432–4444.

TANGA, P., BABIANO, A., DUBRULLE, B. & PROVENZALE, A. 1996 Forming planetesimals in vortices. *Icarus* **121**, 158–170.

TELIB, H. & ZANNETTI, L. 2011 Hollow wakes past arbitrarily shaped obstacles. *J. Fluid Mech.* **669**, 214–224.

ZANNETTI, L. & LASAGNA, D. 2013 Hollow vortices and wakes past Chaplygin cusps. *Eur. J. Mech. (B/Fluids)* **38**, 78–84.